

Galileo GIOVE-A Broadcast E5 Codes and their Application to Acquisition and Tracking

Grace Xingxin Gao, David S. De Lorenzo, Alan Chen, Sherman C. Lo, Dennis M. Akos, Todd Walter and Per Enge
Stanford University

BIOGRAPHY

Grace Xingxin Gao is a Ph.D. candidate under the guidance of Professor Per Enge in the Electrical Engineering Department at Stanford University. She received a B.S. in Mechanical Engineering in 2001 and her M.S. in Electrical Engineering in 2003, at Tsinghua University, Beijing, China. Her current research interests include Galileo signal and code structures, GNSS receiver architectures, and GPS modernization.

David De Lorenzo is a member of the Stanford University GPS Laboratory, where he is pursuing a Ph.D. degree in Aeronautics and Astronautics. He received a Master of Science degree in Mechanical Engineering from the University of California, Davis, in 1996. David has worked previously for Lockheed Martin and for the Intel Corporation.

Alan Chen is a Ph.D. candidate in the Department of Aeronautics and Astronautics at Stanford University. He received an M.S. from that department in 2003 and received his S.B. degree in Aeronautics and Astronautics from MIT in 2001. His current research interests involves UXOs, sensor fusion, autonomous helicopters, and GNSS signals.

Sherman C. Lo is currently a research associate at the Stanford University Global Positioning System (GPS) Laboratory. He is the Associate Investigator for the Stanford University efforts on the Department of Transportation's technical evaluation of Loran.

Dennis M. Akos completed the Ph.D. degree in Electrical Engineering at Ohio University within the Avionics Engineering Center. His research interest include: Global Navigation Satellite Systems (GNSS), Software Defined Radio (SDR), applied/digital signal processing, and Radio Frequency (RF) design. Currently he is an Assistant Professor with the Aerospace Engineering Science Department at University of Colorado at Boulder and holds a visiting professor appointment at Luleå University of Technology and a consulting professor appointment with Stanford University.

Todd Walter is a Senior Research Engineer in the Department of Aeronautics and Astronautics at Stanford University. Dr. Walter received his Ph.D. in 1993 from Stanford and is currently developing WAAS integrity algorithms and analyzing the availability of the WAAS signal. He is a fellow of the ION.

Per Enge is a Professor of Aeronautics and Astronautics at Stanford University, where he is the Kleiner-Perkins, Mayfield, Sequoia Capital Professor in the School of Engineering. He directs the GPS Research Laboratory, which develops satellite navigation systems based on the Global Positioning System (GPS). He has been involved in the development of WAAS and LAAS for the FAA. Per has received the Kepler, Thurlow and Burka Awards from the ION for his work. He is also a Fellow of the ION and the Institute of Electrical and Electronics Engineers (IEEE). He received his Ph.D. from the University of Illinois in 1983.

ABSTRACT

In this paper, we decode the PRN codes of the E5a and E5b signals broadcast by the Galileo GIOVE-A test satellite. The Galileo E5 band overlaps with Distance Measuring Equipment (DME) and Tactical Air Navigation (TACAN) bands. These navigation systems emit high-power pulses, causing severe interference to E5 signals and thus challenging the decoding process. We apply the 1.8 meter dish of the Stanford GNSS Monitor System to receive the satellite signals. The received data are processed in a chain of signal conditioning, Doppler wipeoff, secondary code wipeoff, code sequence demodulation, and code generator derivation.

Two primary code sequences are revealed in each frequency band, E5a-I, E5a-Q, E5b-I, and E5b-Q. The E5 signals have a chip rate of 10.23 Mbps. All four primary codes have a period of 1msec with 10230 bits and are modulated by secondary codes. The secondary code of E5a-I has 20 bits and that of E5b-I has 4 bits. The secondary codes of E5a-Q and E5b-Q are both 100 bits.

In addition to obtaining the code sequences, we also deduce the code generators. This reduces the required receiver memory size from thousands of bits to 56 bits per code sequence, a potentially important consideration of a multiplicity of codes are made available. As a result, the receiver cost can be dramatically decreased. All broadcast E5 primary codes are proven to be truncated 14-order Gold Codes. They can be generated by Linear Feedback Shift Registers, which are completely specified by tap weights and initial states.

We then apply the codes for acquisition and tracking. By using our own software receiver, we are able to successfully acquire and track the GIOVE-A satellite. This is useful for evaluating the performance of the selected codes.

We intend to use the above technique to further evaluate the GIOVE-B and other Galileo signals as they become available.

INTRODUCTION

The first test satellite of the Galileo system, GIOVE-A was launched on December 28, 2005 [1]. It started to broadcast Galileo signals on January 12th, 2006. GIOVE-A is capable of transmitting on two frequencies at one time from an available set of L1, E5 and E6 bands. It was first broadcasting on L1 and E6 bands. Based on our observation, it switched to L1 and E5 bands in August, 2006 for a few weeks and switched back to L1 and E6 frequencies in September, 2006. Since October 25, 2006, it has been again transmitting on L1 and E5 bands. Our previous paper [2] studied the signals and PRN sequences of the initial GIOVE-A transmission on L1 and E6. This paper analyzes the broadcast Galileo E5 signals and extracts their PRN codes.

Unlike its L1 and E6 counterparts, E5 signals at 1176.45 MHz and 1207.14 MHz are exposed to a unique electromagnetic environment created by existing aeronautical system pulsed emitters, especially Distance Measuring Equipment (DME) and Tactical Air Navigation (TACAN) systems. DME provides distance measurement between aircraft and a ground station. TACAN additionally provides azimuth information and is a military system. These navigation systems consist of an airborne interrogator and a ground-based transponder. DME/TACAN operate in four modes (X, Y, W and Z) between 960 MHz and 1215 MHz in an Aeronautical Radionavigation Services (ARNS) band [3]. The ARNS frequency allocation chart in Figure 1 illustrates its overlap with the E5 band. Only the X-mode replies in the 1151-1213 MHz frequency band, and is composed of pulse pairs with an inter-pulse interval of 12 μ s [4]. The DME/TACAN interference degrades the signal-to-interference plus noise ratio (SINR), and makes the E5

decoding process more difficult than decoding L1 and E6 codes.

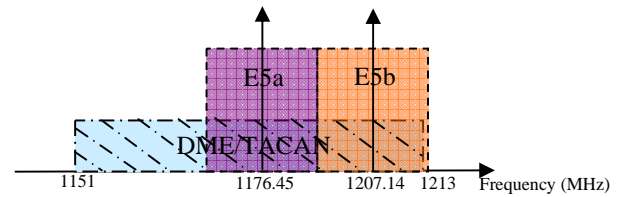


Figure 1. ARNS frequency allocation

The first section of the paper describes the Galileo signal collected from the high gain dish of the Stanford GNSS Monitor System (SGMS) [5]. Strong DME/TACAN pulses are observed in E5a and E5b bands. In the second section, the raw data are conditioned in both time domain and frequency domain to reduce the DME/TACAN interference. In the third section, two codes in each band are discovered, namely, E5a-I, E5a-Q, E5b-I and E5b-Q, following the nomenclature of the ‘Galileo Open Service Signal In Space Interference Control Document (OS SIS ICD) [6]. The code periods are shown to be 1 msec and 10230 bits. Chips in the periodic sequences are estimated from the conditioned I/Q data after wiping off carrier, Doppler offset and a secondary code. In the fourth section, we demonstrate that the code sequences are linear, truncated Gold Codes, so it is only necessary to store the code generators at the receiver. The generators (code polynomials and initial states) are also derived. In the final section, we implement the PRN codes in our software receiver. We demonstrate that our Galileo software receiver can successfully acquire and track the broadcast GIOVE-A signals, and show that, while acquisition and tracking are possible in the presence of DME/TACAN interference, a system that first removes this interference (for example with time-domain pulse blanking) is beneficial.

DATA COLLECTION

The GIOVE-A E5 signals are collected by SGMS, shown in Figure 2. SGMS has a 1.8 m steerable parabolic dish antenna with an L-band feed. The antenna has approximately 7° beamwidth, and provides about 25 dB of gain over conventional patch antennas. The azimuth and elevation motors of the antenna can be driven by satellite tracking software, so that the dish automatically points to and tracks a specific satellite.



Figure 2. Stanford GNSS Monitor System, 1.8m dish

The signal from the feed of the antenna goes through a low noise amplifier, a band pass filter, and is collected by an Agilent 89600 Vector Signal Analyzer (VSA) as shown in Figure 3.



Figure 3. Agilent 89600 Vector Signal Analyzer (VSA)

We also observe the signal on a Hewlett Packard spectrum analyzer.



Figure 4. Observing signal on a HP spectrum analyzer

We use “Nova for Windows”[7] to determine an appropriate observation time for the GIOVE-A satellite pass over Palo Alto, CA, USA, and to drive the antenna to track the GIOVE-A satellite. The interface of the software is shown in Figure 5. It provides the view of satellite paths, azimuth, elevation information, etc.

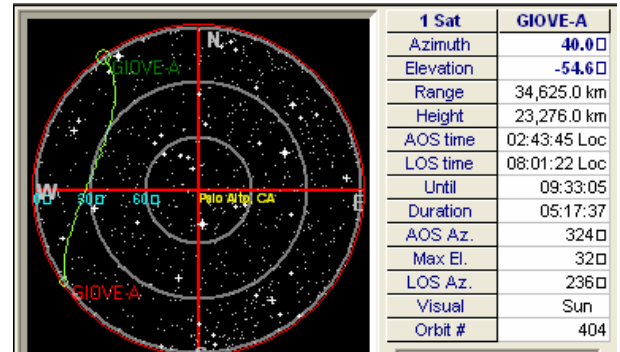
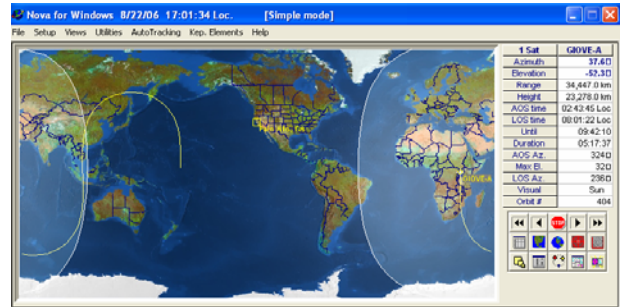


Figure 5. “Nova for Windows” software interface

The VSA data are then uploaded to Matlab. Figures 6 to 9 show the frequency spectra and time-domain plots of the inphase signals of E5a and E5b.

In the frequency-domain plots (Figures 6 and 8), we see strong narrow-band tones attributed to DME, one obvious in the E5a band and three obvious in the E5b band. Each tone represents the airborne interrogators and the beacon DME signal from a nearby airport. The power spectral density of the DME interference exceeds the noise floor of -110 dB by 50 dB for E5a and by 32 dB for E5b. More troubling, it is likely that these observed DME signal were not in the primary beamwidth of the antenna but their strong power levels make them readily apparent in the data. The E5 signals are even weaker than the noise floor and are completely buried in noise, even though the antenna gain is as high as 25 dB. All that is apparent in the spectral density plots is the VSA filter shape and the DME interference. In time domain, we see that strong DME pulses are frequent. They are 5-100 times greater in amplitude than the E5 signals.

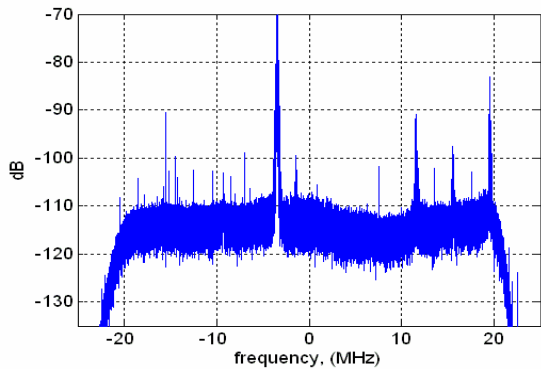


Figure 6. E5a Power spectral density

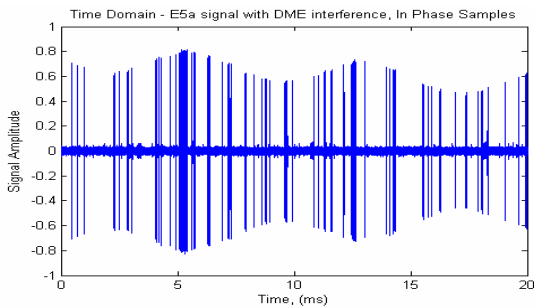


Figure 7. Time domain E5a signal with DME interference, inphase samples

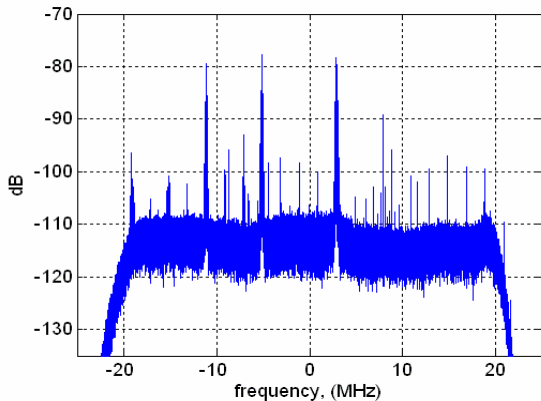


Figure 8. E5b Power spectral density

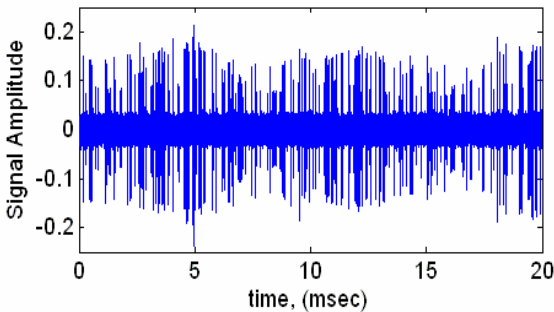


Figure 9. Time domain E5b signal with DME interference, inphase samples

SIGNAL CONDITIONING

Although DME/TACAN signals are strong and cause significant SINR degradation, their pulsed nature, in contrast to the spread spectrum nature of Galileo signals, enables interference mitigation. We apply two methods: pulse blanking in the time domain and notch filtering in the frequency domain.

For brevity, we only present the signal processing results for E5b signals in this paper, as the observed E5b band suffers more interference at the data-collection location than E5a from DME/TACAN. In fact, we apply the same procedures to the E5a signals.

I. Time Domain Conditioning – Pulse Blanking

Figure 10 is a zoomed in version of Figure 9. If we zoom in further, we can see the DME pairs more clearly as shown in Figure 11. The noise amplitude is mostly within 0.03 units, while the DME interference can reach 0.17 units. If the amplitude of the received signal exceeds 0.035, we claim that this part of the signal is corrupted by DME, and set it to zero as shown in Figure 12. This is the time domain method of ‘pulse blanking’.

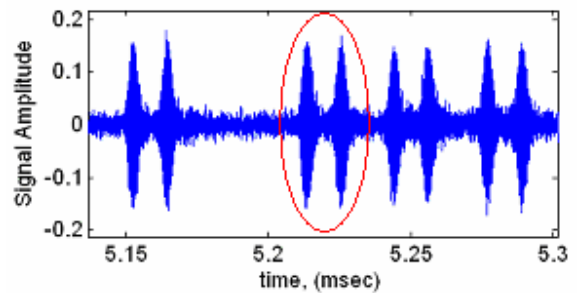


Figure 10. Time domain E5b signal with DME interference, inphase samples, zooming in

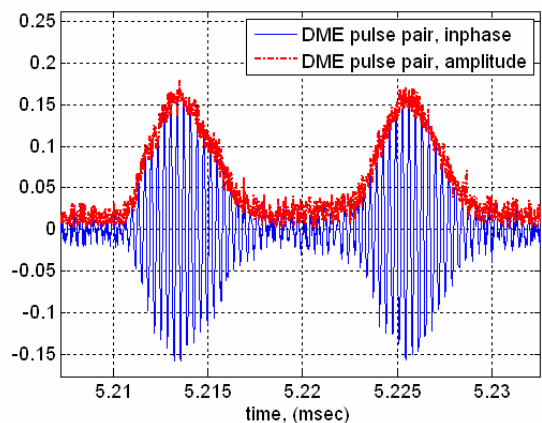


Figure 11. Time domain E5b signal with DME interference, inphase and amplitude

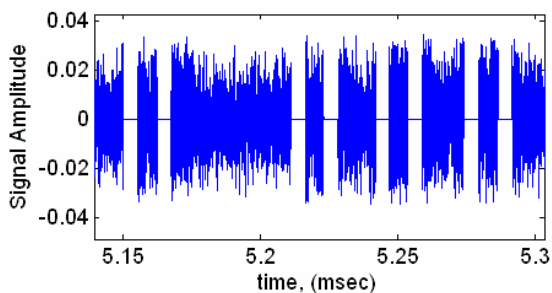


Figure 12. Time domain E5b signal after pulse blanking

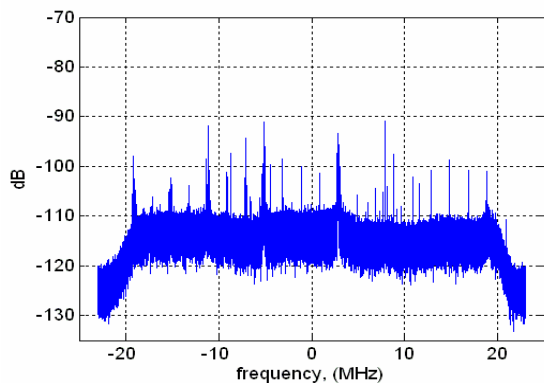


Figure 13. E5b power spectral density estimate, after pulse blanking

Figure 13 shows the power spectrum. Pulse blanking mitigates 13 dB of DME interference, reducing the spikes from -78dB to -91dB. However, smaller spikes still exist at 21 dB above the noise floor. Pulse blanking is effective but not thorough due to the bell shape of the DME pulses. Its tails stretch below the noise floor, and thus cannot be removed simply by pulse blanking alone.

II. Frequency Domain Conditioning – Notch Filtering

In order to further mitigate the DME spikes, notch filtering is applied to the signal. We first transfer the time domain signal to frequency domain by Fast Fourier Transform (FFT). We null the spike frequency components, and then return the frequency expression to the time domain using Inverse Fast Fourier Transform (IFFT). Figures 14 and 15 show the frequency and time domain signals after pulse blanking and notch filtering.

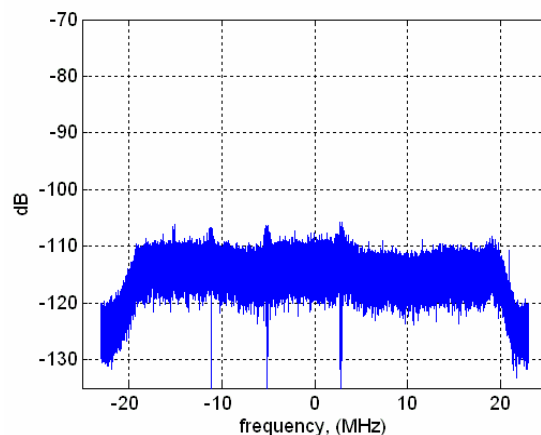


Figure 14. E5b power spectral density estimate, after pulse blanking and notch filtering

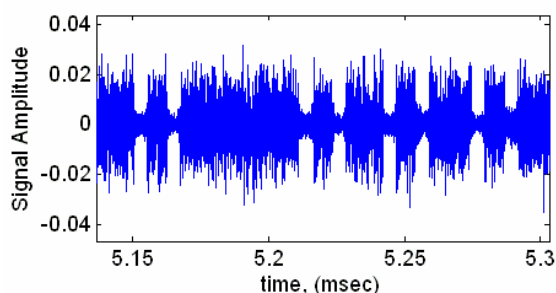


Figure 15. Time domain E5b signal after pulse blanking and notch filtering

Note that in the process of signal conditioning, we lose about 10% of signal energy. However, this loss is very small compared to the interference energy removed; we obtain a net gain in SINR.

CODE SEQUENCE DEMODULATION

The conditioned satellite signal is the product of a carrier, a pseudorandom noise (PRN) code and a secondary code. We now describe each of these components in the following paragraphs.

The carrier frequency is 1207.14 MHz for the E5b signal and 1176.45 MHz for the E5a signal. The relative movement of the satellite with the respect to the Earth causes a Doppler frequency offset associated with the carrier frequency. The Doppler offset results in constant phase variation.

Each of the E5a and the E5b signals has two PRN codes. For each code, there is a low-rate secondary code modulated on top of the carrier and a PRN code. Secondary codes increase the signal repetition time thus reducing the line spectrum in the frequency domain. Since receivers know the secondary codes beforehand, they can integrate for long periods of time for acquisition, and therefore obtain a high processing gain.

The PRN code is the spreading code that satisfies each satellite. Knowing the PRN code is critical for a receiver to perform acquisition and tracking. So far, the broadcast PRN codes are different from the ones released in the Galileo ICD [6].

In order to demodulate the GIOVE-A E5 PRN codes, we need to wipe off the carrier and Doppler offset from the received signal, and extract the secondary codes.

I. Code Period Calculation

We first correlate the whole code sequence with a small slice of itself. The correlation plot is shown in Figure 16. Figure 17 and 18 are the zoomed-in plots of the inphase and quadrature part of the correlation. The intervals between pairs of peaks are used to compute the code length. As the peaks occur at multiples of 1 msec, the PRN codes have period of 1 msec.

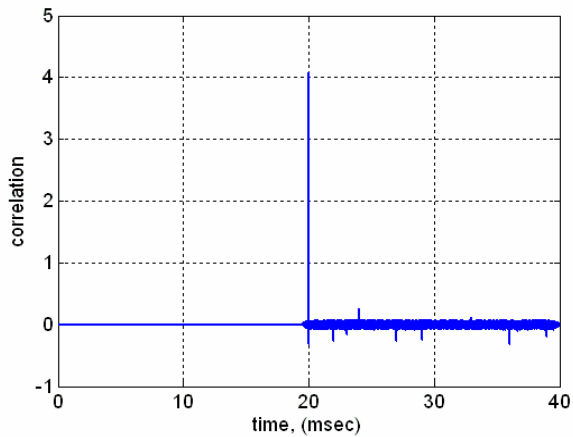


Figure 16. Correlation of the whole code sequence with a small slice of itself

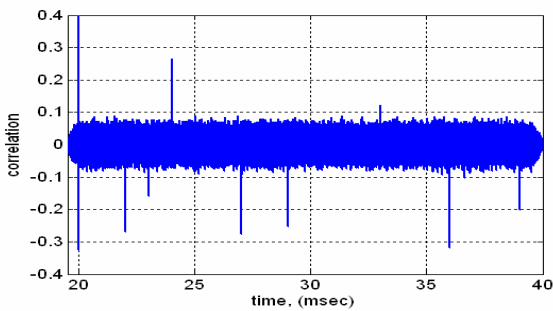


Figure 17. Correlation of the whole code sequence with a small slice of itself, inphase

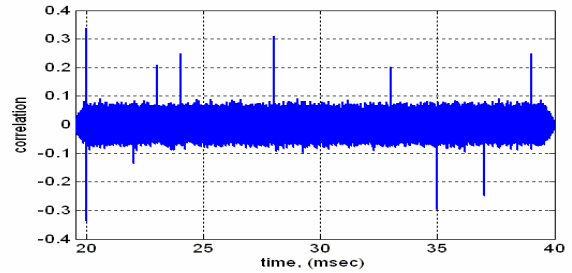


Figure 18. Correlation of the whole code sequence with a small slice of itself, quadrature

II. Doppler Wipeoff

The Doppler offset has two effects on the correlation peaks. It results in constant phase variation, creating peaks in the inphase and quadrature channels. Moreover, it modulates the real and imaginary parts with a cosine and sine wave, respectively, causing the peak heights to vary.

In order to remove the Doppler offset, we search the whole Doppler domain from -5000 Hz to 5000 Hz and minimize the peak height variation after Doppler compensation.

After wiping off the Doppler and adjusting the initial phase, we can see peaks with more uniform heights in the inphase channel and no peak in the quadrature channel. This verifies the correctness of Doppler offset estimate.

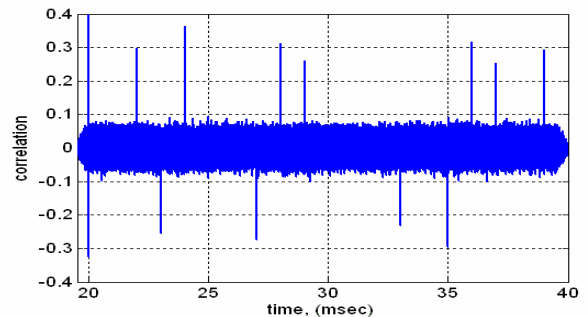


Figure 19. Correlation of the whole code sequence with a small slice of itself, inphase, after Doppler removal

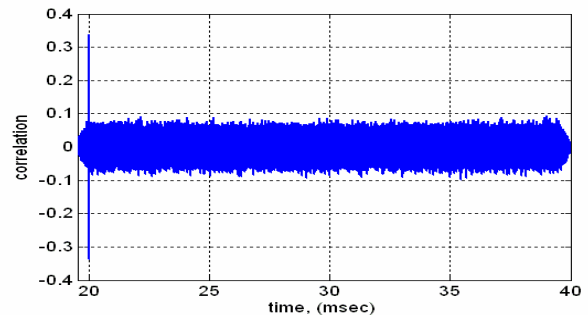


Figure 20. Correlation of the whole code sequence with a small slice of itself, quadrature, after Doppler removal

III. Secondary Code Wipeoff

At multiples of 1 msec, we deduce null peaks where no positive or negative peaks exist. We now assume the small slice of code used for correlation contains $(E5b-I)+(E5b-Q)$ in order to extract the secondary code; we discuss this assumption later. To avoid bit transition within the small slice of data, we choose the slice length to be 0.5 msec; compute two consecutive slices of 0.5 msec and use the one with relatively larger peaks. Then the positive peaks represent $[(E5b-I) + (E5b-Q)]$, the negative peaks represent $-[(E5b-I) + (E5b-Q)]$, while the null peaks can be either $[(E5b-I) - (E5b-Q)]$ or $-[(E5b-I) - (E5b-Q)]$. To solve the ambiguity of the null peaks, we pick another slice of data that corresponds to a null peak. We assume this second slice of data contains $[(E5b-I) - (E5b-Q)]$. We correlate it with the whole sequence. We again see positive and negative peaks and null peaks. This time, the positive peaks stand for $[(E5b-I) - (E5b-Q)]$ and the negative peaks are $-[(E5b-I) - (E5b-Q)]$. The null peaks are either $[(E5b-I) + (E5b-Q)]$ or $-[(E5b-I) + (E5b-Q)]$. Figure 21 illustrates the relationship between peaks and the secondary code bits. The positive blue peaks and positive red peaks correspond to '+1' for E5b-I secondary code; the negative blue peaks and negative red peaks correspond to '-1' for E5b-I secondary code. The positive blue peaks and negative red peaks correspond to '+1' for E5b-Q secondary code; the negative blue peaks and positive red peaks correspond to '-1' for E5b-Q secondary code. Table 1 shows the reading of secondary codes in the example shown in Figure 21.

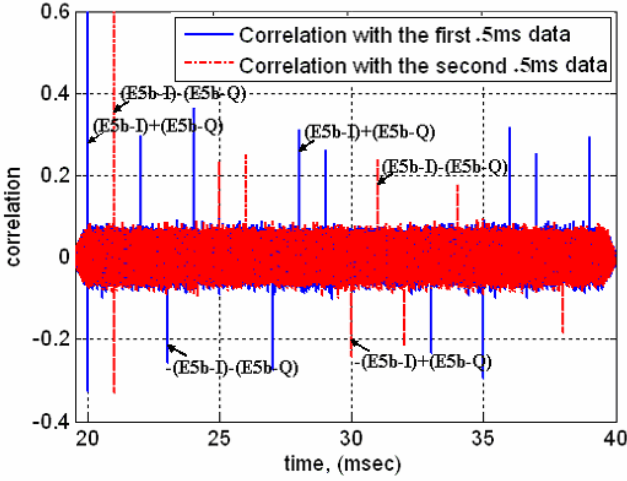


Figure 21. Extracting secondary code bits according to correlation peaks

	Period	Secondary code
E5b-I code	10230	[1, 1, 1, -1, 1, 1, 1, -1, 1, 1, -1, 1, -1, -1, 1, -1, 1, 1, -1, 1...]
E5b-Q code	10230	[1, -1, 1, -1, 1, -1, -1, -1, 1, 1, 1, -1, 1, -1, -1, -1, -1, 1, 1, 1...]

Table 1. Secondary code reading of E5b-I and E5b-Q based on Figure 21

Once the secondary code is known, we coherently stack multiple slices of the code sequences and obtain clean $(E5b-I)+(E5b-Q)$ and $(E5b-I)-(E5b-Q)$ signals. We then unmix the PRN codes for E5b-I and E5b-Q, as follows. $E5b-I = \{[(E5b-I)+(E5b-Q)] + [(E5b-I)-(E5b-Q)]\}/2$; $E5b-Q = \{[(E5b-I)+(E5b-Q)] - [(E5b-I)-(E5b-Q)]\}/2$.

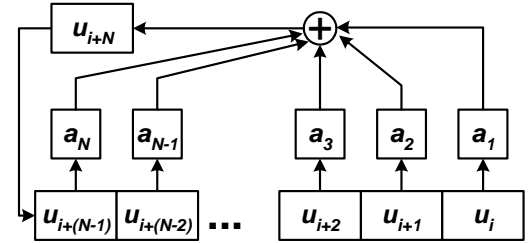
DERIVING CODE GENERATORS

With the code sequences for E5b band obtained, we can implement these PRN sequences in Galileo receivers for acquisition and tracking. However, storing thousands of bits in the receiver is expensive for flash memory. For DSP units, the memory cost is even greater. This drives the desire to minimize the code representation.

We consider linear codes as likely candidates for the Galileo code design, because they have good correlation performance, and can be generated by linear feedback shift registers (LFSR), which require only tens of bits.

The schematic of a LFSR is shown in Figure 22. Its outputs are linear combinations of the previous bits. In other words, the output sequence is completely determined by its tap weights $(a_1 \dots a_N)$ and initial state

$(u_1 \dots u_N)$. The LFSR arithmetic is modulo 2.



$$u_{i+N} = a_N * u_{i+(N-1)} \oplus a_{N-1} * u_{i+(N-2)} \oplus \dots \oplus a_2 * u_{i+1} \oplus a_1 * u_i$$

Figure 22. Linear Feedback Shift Register (LFSR)

The algorithm in Figure 23 is developed for searching for a linear code representation.

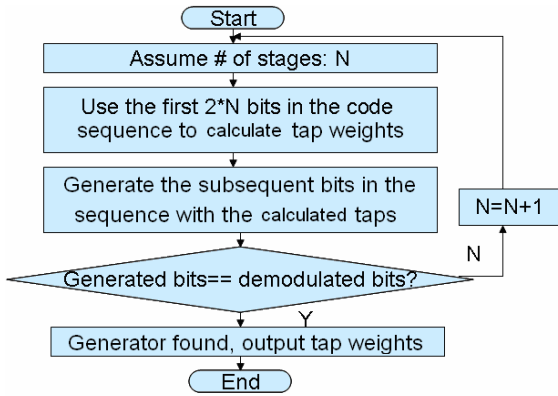


Figure 23. Searching for linear code representation

Take the E5b-I code as an example. Since the code has period 10230 bits, if it was a linear code, the number of stages must exceed $\log_2(10230)$. We initialize $N=14$. We can form the following equation set with 14 equations, and 14 unknown tap weights, $a_1 \dots a_{14}$.

$$\begin{cases} u_{15} = a_{14} \cdot u_{14} \oplus a_{13} \cdot u_{13} \oplus \dots \oplus a_1 \cdot u_1 \\ u_{16} = a_{15} \cdot u_{15} \oplus a_{14} \cdot u_{14} \oplus \dots \oplus a_2 \cdot u_2 \\ \dots \\ u_{28} = a_{27} \cdot u_{27} \oplus a_{26} \cdot u_{26} \oplus \dots \oplus a_{14} \cdot u_{14} \end{cases}$$

The above equation set is solved modulo 2 to obtain the tap weights. The following bits in the sequence can then be generated.

If the generated bits and the demodulated bits match, the code generator is then found. If not, we increment N and repeat.

With this algorithm, both E5b-I code and E5b-Q codes are proven to be linear codes, and they can both be generated by 28-order LFSRs. The 28-order polynomials can be further factorized into two 14-order polynomials. This indicates that the E5b-I and E5b-Q code sequences can be generated by modulo 2 summing the outputs of two 14 stage LFSRs. In fact, the two 14-order polynomials form the preferred pair of a Gold Code [8].

Recall that in the previous section, we used a small slice of code to correlate with the whole code sequence. We made the assumption that the small slice of the code contains (E5b-I)+(E5b-Q). This assumption may not be true. In fact, the small slice of code can be any linear combination of E5b-I and E5b-Q code. Since we assume it is (E5b-I)+(E5b-Q), all the secondary code bits are possibly flipped. As a result, after wiping off the secondary code, the whole E5b-I or E5b-Q sequence can be flipped. This ambiguity can be solved after deriving the PRN code polynomials. If the PRN code polynomial can be factorized by '1+X', then the code is flipped.

Otherwise, it is not. This is because the polynomial '1+X' generates a sequence of all '1's that is added modulo 2 to the code sequence, flipping all code bits.

E5b-I and E5b-Q are concluded to be 14-stage Gold codes. The polynomials and initial states are listed below.

E5b-I code (10230 bits, 1msec, 14-stage Gold code)	
Polynomial_1	$X^{14}+X^{13}+X^{11}+X^4+1$
Initial State_1	[1 1 1 1 1 1 1 1 1 1 1 1 1 1]
Polynomial_2	$X^{14}+X^{12}+X^9+X^8+X^5+X^2+1$
Initial State_2	[1 1 1 0 0 0 1 0 1 0 0 0 1 0]
E5b-Q code (10230 bits, 1msec, 14-stage Gold code)	
Polynomial_1	$X^{14}+X^{13}+X^{11}+X^4+1$
Initial State_1	[1 1 1 1 1 1 1 1 1 1 1 1 1 1]
Polynomial_2	$X^{14}+X^{12}+X^9+X^8+X^5+X^2+1$
Initial State_2	[1 1 0 0 0 0 0 0 0 0 0 1 0 0]

Table 2. Galileo E5b code generators

We apply the same method for E5a signals. The E5a-I and E5a-Q code generators are also obtained by the algorithm in Figure 23. They are shown to be Gold codes as well. The polynomials and initial states are shown in Table 3.

E5a-I code (10230 bits, 1msec, 14-stage Gold code)	
Polynomial_1	$X^{14}+X^8+X^6+X+1$
Initial State_1	[1 1 1 1 1 1 1 1 1 1 1 1 1 1]
Polynomial_2	$X^{14}+X^{12}+X^8+X^7+X^5+X^4+1$
Initial State_2	[1 1 1 0 1 0 1 0 1 1 1 1 1 1]
E5a-Q code (10230 bits, 1msec, 14-stage Gold code)	
Polynomial_1	$X^{14}+X^8+X^6+X+1$
Initial State_1	[1 1 1 1 1 1 1 1 1 1 1 1 1 1]
Polynomial_2	$X^{14}+X^{12}+X^8+X^7+X^5+X^4+1$
Initial State_2	[0 1 1 0 1 1 0 0 1 0 1 0 1 0]

Table 3. Galileo E5a code generators

APPLYING THE CODES FOR ACQUISITION AND TRACKING

With the decoded E5a and E5b PRN codes, signals from the GIOVE-A test satellite are acquired and tracked with a multi-signal all-in-view GNSS software receiver implemented in MATLAB™ (Figure 24; [9] [10]). In addition to the E5 signal, this receiver is also capable of signal acquisition and tracking of GPS C/A-code, pseudo-P-code (simulated signals only), or Galileo L1 or E6 codes from the GIOVE-A test satellite.

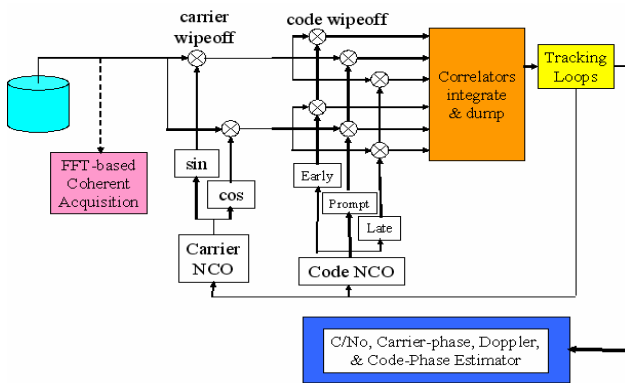


Figure 24. Software receiver block diagram

Acquisition is implemented as a parallel code-phase search using FFT-based processing. Several milliseconds of data may be combined to increase weak-signal sensitivity or to provide more accurate estimates of carrier Doppler frequency, although at a trade-off in execution time.

Immediately after acquisition, the code-phase and carrier-frequency estimates are used to initialize the code and carrier numerically-controlled oscillators (NCOs). The receiver refines the estimates of carrier frequency, carrier phase, and code phase through a succession of tracking modes, where the phase-lock and delay-lock loop noise bandwidths are successively reduced. These estimates are shown in Table 4. Since one of the tracking objectives was the estimation of the secondary code length and sequence, integration times were kept to 1msec for all tracking modes (the length of the primary spreading code sequence) – this is because carrier polarity may change at each millisecond, and this sequence is unknown until the secondary decoding has occurred.

We load the raw GIOVE-A data collected through the SGMS dish to our software receiver. We first pass the data into the acquisition module. The 3-D acquisition plot in Figure 25 shows the normalized correlation function output as a function of code phase on one axis and carrier Doppler frequency on the other axis. We read the code-phase and Doppler estimate based on the location of the main peak in the code phase and Doppler domain. The correlation peak to next peak ratio (CPPR) is only 6.24dB. This reflects the SINR degradation due to DME pulses. The Doppler estimate is -700 Hz. Due to the low CPPR, this estimate can be inaccurate and can cause converging failure in the next tracking module.

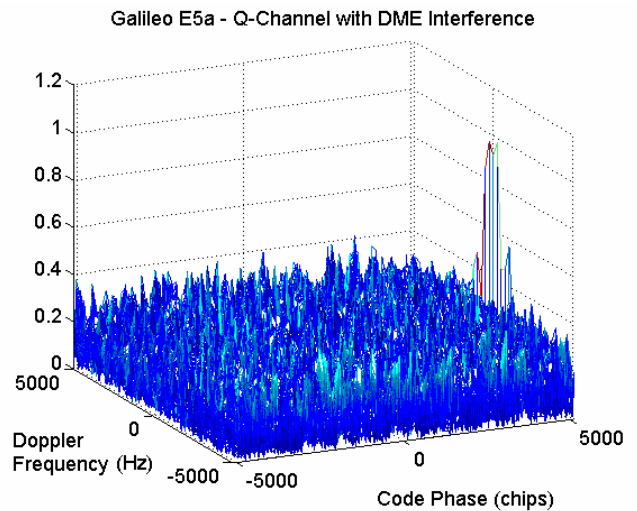


Figure 25. Acquisition plot of Galileo E5a-Q channel

We then feed the code-phase and carrier-frequency information to the tracking module as an initial estimate. The tracking output in Figure 26 shows four subplots as follows, each as a function of elapsed tracking time along the horizontal axis:

- Upper-left: Phase Lock Loop (PLL) discriminator output in degrees
- Upper-right: Delay Lock Loop (DLL) discriminator output in meters
- Lower-left: carrier Doppler frequency estimate
- Lower-right: code-phase estimate with respect to the receiver's on-board millisecond counter

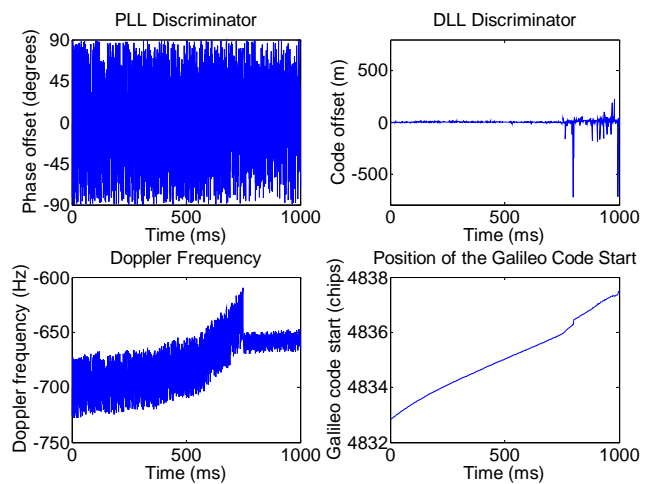


Figure 26. Tracking results of E5a-Q channel

Unfortunately, the PLL and DLL are not locked. We observe excessive jumps in the estimates of phase offset and code offset. This is caused by inaccurate Doppler and code-phase output from the acquisition module due to the strong DME interference. However, it is possible that a more robust tracking implementation, including a use of a

Frequency Lock Loop (FLL) would improve convergence performance.

To solve this problem, we applied pulse blanking before sending the raw data into the acquisition module. Figure 27 shows the acquisition results for E5a-I and E5a-Q channels. The integration time remains unchanged. This time, we see less noisy plots. The CPPR is increased from 6 dB to 19 dB by the pulse blanking technique. The Doppler estimate is now -420 Hz.

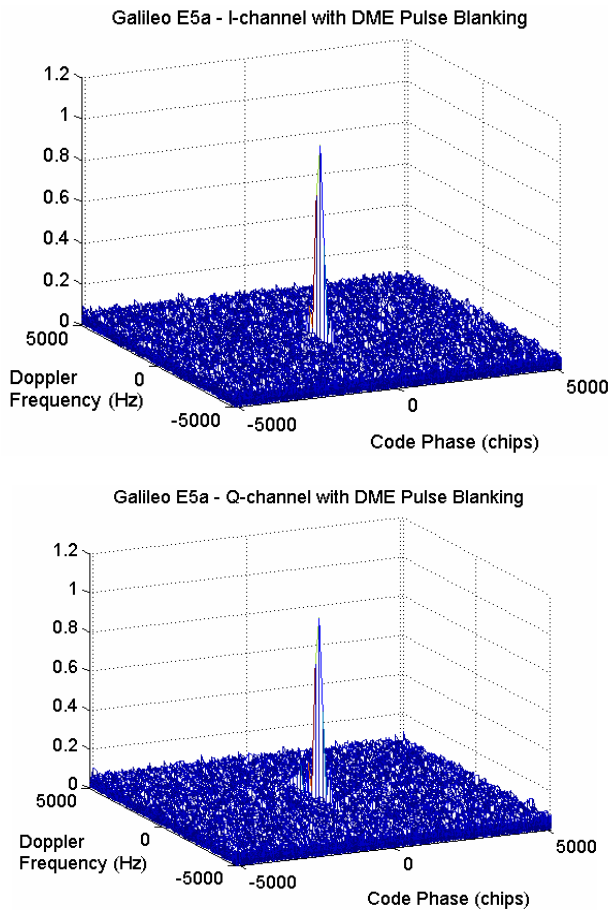


Figure 27. Acquisition plot of Galileo E5a-I and E5a-Q channels with pulse blanking

Next, we initialize the tracking loops with the new code-phase and Doppler estimates. The tracking results of E5b-I and E5b-Q are shown in Figure 28 and 29 respectively.

With pulse blanking technique, the PLL and DLL are locked. All tracking outputs converge, such as phase offset, code offset and Doppler frequency. The PLL and DLL discriminators settle within 100 msec.

The Doppler frequency is locked at -450 Hz as shown in the lower-left plots in Figures 28 and 29. Recall that in the non-pulse-blanking case, the Doppler estimate from the

acquisition module is -700 Hz, which is wrong by 250 Hz. This makes the DLL and PLL incorrectly lock onto -650 Hz as shown in the lower-left plot in Figure 26, causing periodic large discriminator errors.

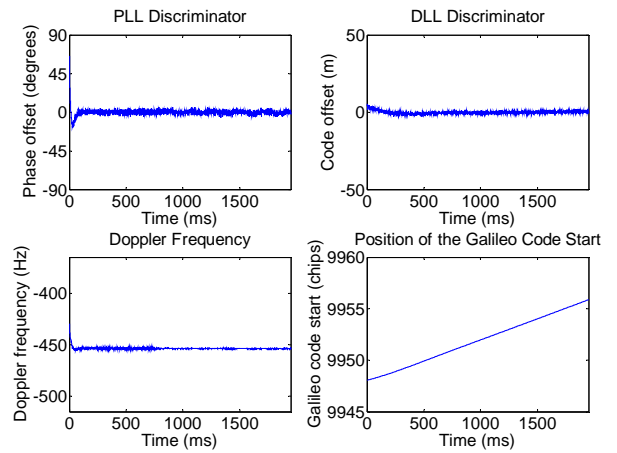


Figure 28. Tracking results of E5a-I channel with pulse blanking

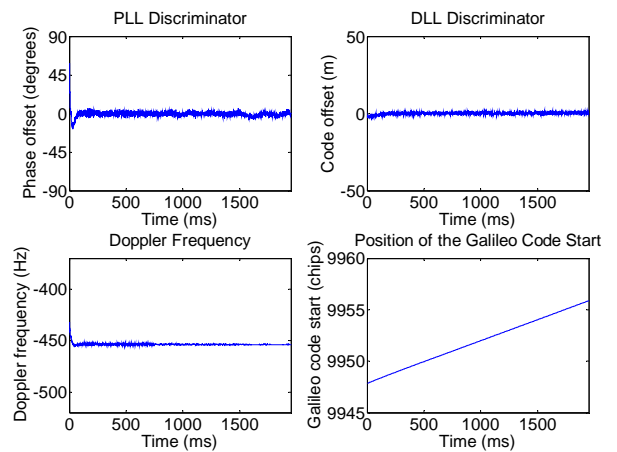


Figure 29. Tracking results of E5a-Q channel with pulse blanking

For brevity, we only show the acquisition and tracking results for E5a channel. The results for E5b are similar.

The software receiver also outputs secondary codes for all channels as follows.

- E5a-I, 20 bits
[1 -1 -1 -1 -1 -1 -1 -1 -1 -1 -1 1 1 1 1 -1 1 -1 -1 1]
- E5a-Q, 100 bits
[1 1 1 1 -1 1 1 1 -1 1 -1 1 -1 1 -1 1 -1 1 -1 1 -1 1
1 1 1 1 -1 -1 -1 1 1 1 -1 -1 -1 1 1 -1 -1 1 1 -1 -1 1
1 -1 -1 1 1 -1 1 1 -1 -1 -1 1 1 -1 1 1 1 -1 -1 -1 -1
1 -1 -1 1 1 -1 1 1 -1 -1 -1 1 1 -1 1 1 1 -1 1 -1 -1
1 -1 -1 1 1 -1 1 1 1]
- E5b-I, 4 bits
[-1 -1 -1 1]

- E5b-Q, 100 bits
 [1 -1 -1 -1 1 1 1 1 -1 1 1 -1 1 1 1 -1 -1 -1 -1 1 -1 1
 -1 1 -1 1 -1 -1 -1 -1 -1 1 1 -1 -1 -1 1 1 1 1 1 1 -1 1
 1 1 -1 -1 -1 1 1 -1 -1 1 -1 -1 1 1 -1 1 1 -1 -1 -1 1
 1 1 -1 -1 1 -1 -1 -1 -1 1 1 1 1 1 1 -1 1 1 -1 1 1
 1 1 -1 1 1 -1 1 -1 -1 1 1 1 -1 1]

CONCLUSION

This paper decodes the Galileo E5 PRN sequences that are broadcast by the GIOVE-A satellite. Not only are the code bits obtained, but also the code generators have been derived. All codes, E5a-I, E5a-Q, E5b-I and E5b-Q, are proven to be truncated Gold Codes, and can be generated by linear feedback shift registers. The E5a-I and E5b-I codes carry secondary codes of 20 msec and 4 msec respectively; E5a-Q and E5b-Q have secondary codes of 100 msec. A summary of the codes is listed in Table 5.

GIOVE-A broadcast codes			Type	Length	Period	Generated by	With data?
E5a codes	E5a-I	Primary	Truncated Gold code	10230	1 msec	Two 14-stage LFSRs	No
		Secondary		20	20 msec		
	E5a-Q	Primary	Truncated Gold code	10230	1 msec	Two 14-stage LFSRs	No
		Secondary		100	100 msec		
E5b codes	E5b-I	Primary	Truncated Gold code	10230	1 msec	Two 14-stage LFSRs	No
		Secondary		4	4 msec		
	E5b-Q	Primary	Truncated Gold code	10230	1 msec	Two 14-stage LFSRs	No
		Secondary		100	100 msec		

Table 4. Summary of Galileo broadcast E5 codes

We successfully acquire and track the GIOVE-A satellite by implementing E5 codes into our own software receiver. The approximately code phase and carrier frequency estimates are obtained through acquisition, and are used to initialize the code and carrier NCOs in tracking. The refined estimates of carrier frequency, carrier phase, and code phase are obtained through a succession of tracking modes. With no interference mitigation technique, the tracking loops do not converge in all cases; the tracking loops consistently converge when pulse blanking is applied to the raw data before the acquisition module. Therefore, interference mitigation is desirable and beneficial for Galileo E5 signals.

ACKNOWLEDGMENTS

The authors gratefully acknowledge the support of the Federal Aviation Administration under Cooperative Agreement 95-G-005. This paper contains the personal comments and beliefs of the authors, and does not

necessarily represent the opinion of any other person or organization.

REFERENCES

[1] European Space Agency, ‘Successful launch of the Galileo Satellite: GIOVE-A, the First European Navigation Satellite in Space’, December 28, 2005. Document can be found on-line at: <http://www.galileoju.com/doc/8541%20Press%20Release%20Successful%20Launch%20of%20GIOVE%20A.pdf>

[2]. Grace Xingxin Gao, Jim Spilker, Todd Walter, Per Enge and Anthony R Pratt, ‘Code Generation Scheme and Property Analysis of Broadcast Galileo L1 and E6 Signals’, ION GNSS conference, Fort worth, TX, September 2006

[3]. Taehwan Kim, Joe Grabowski, ‘Validation of GPS L5 Coexistence with DME/TACAN and Link-16 System’, ION GNSS conference, Portland, OR, September 2003

[4]. Frederic Bastide, Eric Chatre, Christophe Macabiau, Benoit Roturier, ‘GPS L5 and Galileo E5a/E5b Signal-to-Noise Density Ratio Degradation Due to DME/TACAN signals: Simulation and Theoretical Derivation’, ION NTM Conference, San Diego, CA, January, 2004

[5] Sherman Lo, Dennis Akos, Thomas Grelier, Alan Chen, Grace Gao, Joel Dantepal and Jean-luc Issler, ‘GNSS Album, Images and spectral signatures of the new GNSS signals’, Inside GNSS Magazine, June 2006

[6] European Space Agency and Galileo Joint Undertaking, ‘Galileo Open Service Signal In Space Interference Control Document (OS SIS ICD)’, May 23, 2006. Document can be found on-line at: <http://www.galileoju.com/page2.cfm>

[7] <http://www.dxzone.com/cgi-bin/dir/jump2.cgi?ID=3717>

[8] Solomon W. Golomb and Guang Gong, ‘Signal Design for Good Correlation’, Cambridge University Press, 2005

[9] D.S. De Lorenzo, J. Rife, P. Enge, and D.M. Akos, 2006, ‘Navigation Accuracy and Interference Rejection for an Adaptive GPS Antenna Array,’ Proc. ION GNSS 2006

[10] K. Borre, D.M. Akos, N. Bertelsen, P. Rinder, and S.H. Jensen, ‘A Software-Defined GPS and Galileo Receiver: A Single-Frequency Approach’, Birkhauser, 2006